 IEEE Transactions on Nuclear Science, Vol. NS-30, No. 4, August 1983

STATUS REPORT ON THE NORMAL CONDUCTING CW RACETRACK MICROTRON CASCADE "MAMI"

H. Herminghaus, B. Dreher, H. Futeneuer, K.H. Kaiser, M. Kelliher*, R. Klein, H.J. Kreidel, M. Loch, U. Ludwig-Mertin, K. Merle, H. Schoeler, R. Schulze, P. Semmel, G. Stephan.
Institut für Kernphysik, Universität Mainz, 6500 Mainz, W.-Germany
*University of Glasgow, U.K.

Summary

At present, the first two stages (175 MeV) of the three-stage c.w. microtron cascade MAMI have been completed. The report concentrates on the design of the 2nd stage, which had been completed by the end of 1982 and which, so far, has not yet been described in detail elsewhere. First beam had been obtained by Feb. 1983, best beam transmission obtained so far is in excess of 94%, maximum extractable energy achieved so far is 187 MeV.

General

The general scheme and the main data of MAMI are compiled in Fig. 1 and Tab. 1. Stages I und II have now been completed. A final decision on funding of the third stage is expected by fall 1983. As compared to earlier versions (e.g. [1],[2]) the nominal output energy of the 2nd stage has been raised from 100 to 175 MeV (essentially by adding another klystron). This is helpful to lower the influence of synchrotron quantum fluctuations in the 3rd stage. Further, it allows us to do experiments above the pion threshold prior to installation of the 3rd stage already.

The first stage (14 MeV) has been in operation since spring 1979 for about 2300 hours, thereof about 1500 hours for machine tests, the rest for originally unforeseen user's experiments ([2],[3],[4]). Especially the latter runs, when the machine was operated by the users groups, nicely demonstrated the reliability of the machine which in most cases showed perfectly stable operation over several hours. This machine and it's behaviour have been described in some detail elsewhere (e.g. [2],[5],[6],[7],[8],[9]), so the present paper will concentrate more or less on the 2nd stage.

	stage	I	II	III
General				
input energy	[MeV]	2.1	14	175
output energy	[MeV]	14	175	840
number of traversals		20	51	74
total power consumpt.	[kW]	280		900
Magnet System				
magnet distance	[m]	1.66	5.59	11.83
magnetic field	[T]	0.1	0.54	1.54
max. orbit diameter	[m]	0.97	2.17	3.65
magnet weight (each)	[t]	1.3	43	305
gap width	[cm]	6	7	12
RF-System				
number of klystrons		2		5
linac length	[m]	0.8	3.55	10.4
total rf power	[kW]	9	64	197
beam load	[kW]	1.2	16	67
energy gain per turn	[MeV]	0.59	3.16	9.0
Beam Performance (design, at 100 µA)				
energy width	[keV]	±9	±18	±60
emittance vert.	mm*mrad	0.17 π	0.04 π	0.01 π
emittance hor.	mm*mrad	0.17 π	0.09 π	0.14 π
Status		operating		not yet funded

Injector: at present van de Graaff, later injector linac

Klystrons: Thomson-CSF TH 2075, 50 kW c.w., η=60%

Frequency: 2449.3 MHz

Tab. 1: Main parameters of MAMI

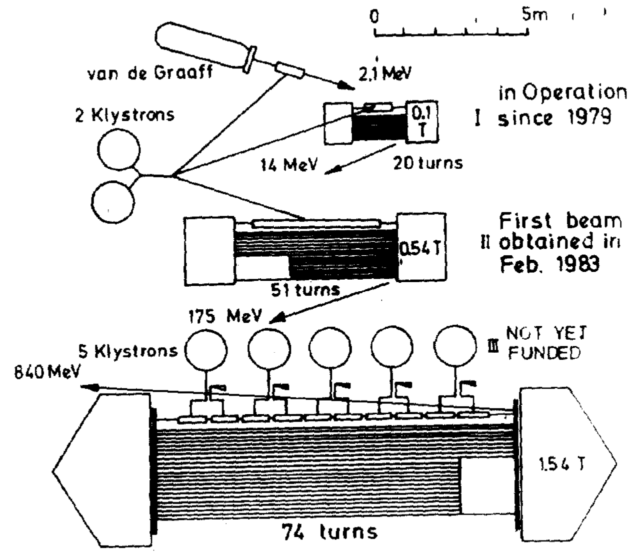

Fig. 1: Scaled scheme of the MAMI project

Design and Technical Details of the 175 MeV-Stage

Beam Guiding System

The beam transport system [10] shown in Fig. 2 has to match the six-dimensional phase space of the beam leaving the 14 MeV-microtron to the acceptance of the second stage. The parameters of the first "chicane-like" part of the system are chosen in such a way that the transverse beam dispersion at the output of the first microtron is canceled. The following matching section (identical to the RTM1-section) makes use of its debunching effect to adjust the energy spread in the beam while the bunch length is reduced to it's correct value by the longitudinal dispersion of the second part of the magnet system. For the vertical phase space matching which requires a beam waist 0.75 m in front of the second end magnet the focusing and defocusing effects of the inclined dipole edges are used together with the quadrupole triplett Q5-Q7. Due to the fact that all pole edges are normal to the RTM-axes the dipole system acts horizontally like a drift space. The matching in this plane is done in a nearly decoupled way with quadrupole Q4 located at a vertical waist (the triplett Q5-Q7 introduces no horizontal focusing).

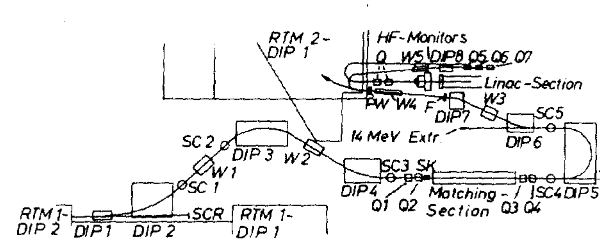

Fig. 2: Scaled scheme of the transport system between RTM1 and RTM2 (DIP: dipole; Q: quadrupole; Sc: movable wire scanner; PW: pick-up wire for large beam displacements; SCR: view screen; SK: protecting collimator; W: vert. steering magnet; F: ferrite intensity monitor)

0018-9499/83/0800-3274$01.00© 1983 IEEE

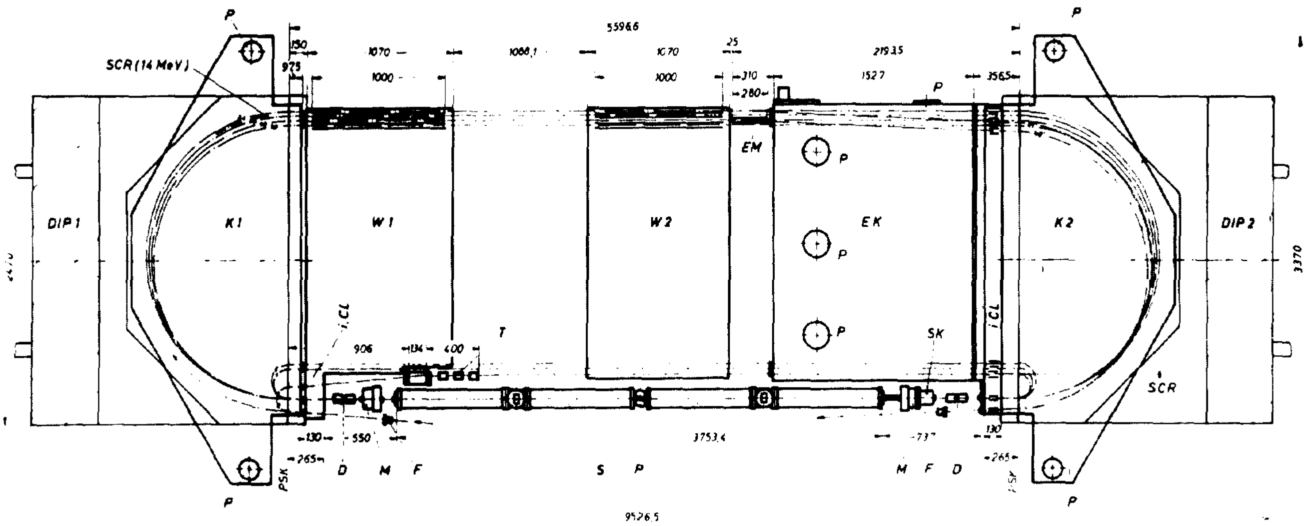

Fig. 3: Scaled scheme of the RTM2 beam guiding system

The beam guiding system of the 175 MeV microtron shown in Fig. 3 consists of the following parts: the two 180°-dipoles, the beam line, the two arrays of correcting dipoles W1 and W2, the inactiv field clamps ICL, the movable extraction magnet EM and the RTM2-vacuum system.

For beam focusing quadrupole doublets D are located on the linac axis near the 180°-magnets separated by inactive field clamps ICL. In this focusing scheme the adiabatic damping by the increase of particle energy and the decay in focusing strength combine in such a way that the beam size stays nearly constant during acceleration while the beam divergence is proportional to the inverse of its energy. The horizontal and vertical β-functions start with 3.1 and 3.7 m respectively at 14 MeV and end up with 51 and 59 m respectively at 175 MeV.

The correcting dipoles W1 and W2 consist of rectangular μ-metall boxes of 1 m length for each turn containing two pairs of one-layer coils in window frame configuration for horizontal and vertical beam deflections of about ± 1 mrad. Corresponding to the experience made with the 14 MeV-stage the deflecting capability is increased at the low energy turns. The upper and lower part of the boxes are made from common plates which simultaneously represent the poles of inactive clamp ICL for DIP1 in case of W1. For DIP2 a shorter but otherwise identical inactive clamp is installed behind the extraction chamber EK.

For extraction the beam is deflected in direction to the linac axis by 43 mrad in front of EK from the return path chosen. Thus, a displacement of twice the spacing between the return paths is produced in front of DIP2. Of course, the same displacement is obtained with respect to the common axis after bending.

The vacuum system is made from aluminium and consists of the magnet chambers K1 and K2, the extraction chamber EK and the 51 beam pipes between K1 and EK.

Due to the necessity to protect the chambers against the atmospheric pressure by spacers and to shield the beams against the long range fringe field of the magnets by μ-metall boxes in EK only every second turn can be extracted starting from turn number 3.

The microtron magnets [11], schematically shown in Fig. 4, are homogeneous magnets with a reverse field stripe parallel to the front edges for the compensation of vertical fringe field defocusing.

Following the operational experience with the 14 MeV stage the magnet position can be optimized remotely in it's three angular coordinates during microtron operation.

In order to determine the current distribution for the pole face correction coils the field distributions were measured near the upper and lower pole surfaces

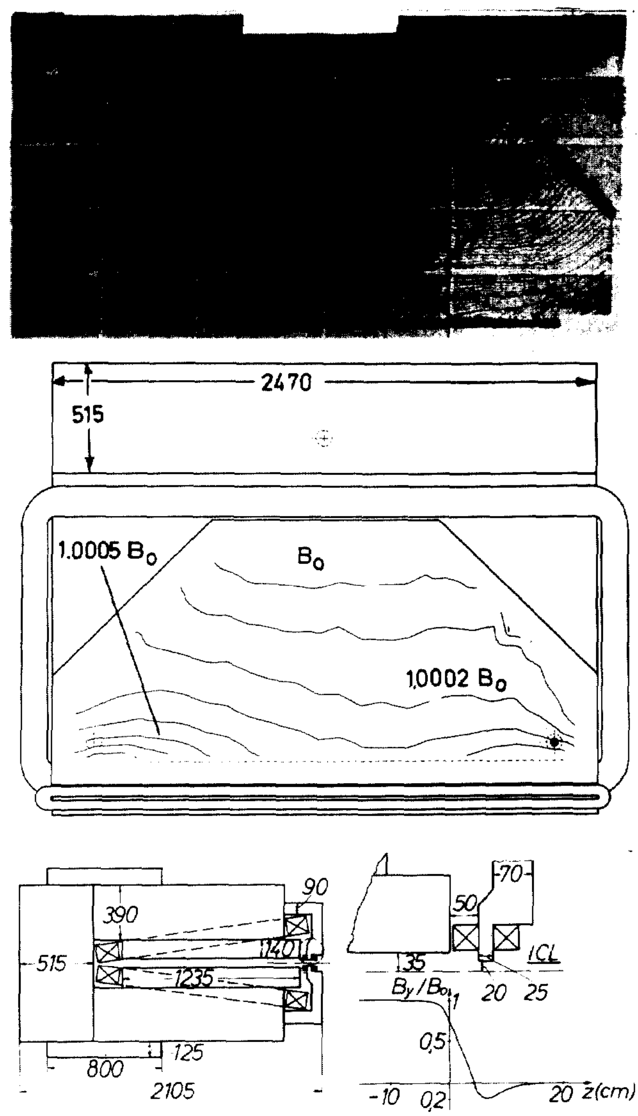

Fig. 4: Schematic drawing of the RTM2 end magnets with fringe field and the constant field line distribution for DIP2 before and after correction

for 0.57 and 0.54 tesla. Then, one set of correcting coils was produced for 0.57 tesla (185 MeV output energy) and another set takes account of the difference in the two field distributions. Under the assumption that the difference of the field configurations changes only linearly in the neighbourhood of 0.57 tesla the inhomogeneity at 0.61 tesla is compensated if the current in the second coil set is simply reversed.
In Fig. 4 the constant field lines in DIP2 are shown without and with correction by the pole face windings. All measurements were done after a special cycling procedure for the coil current in order to obtain a reproducable field distribution.

Accelerating Structures and RF-System

The altogether 4.4 m of accelerating structure (biperiodic on-axis coupled structure [12]) for stage II we fabricated ourselves [13].
The linac of stage II consists of two 1.77 m long sections, each bolted together from three parts by a special combined vacuum-rf-seal (Fig. 5) located at the accelerating cavities neighbouring the input-coupler on both sides.

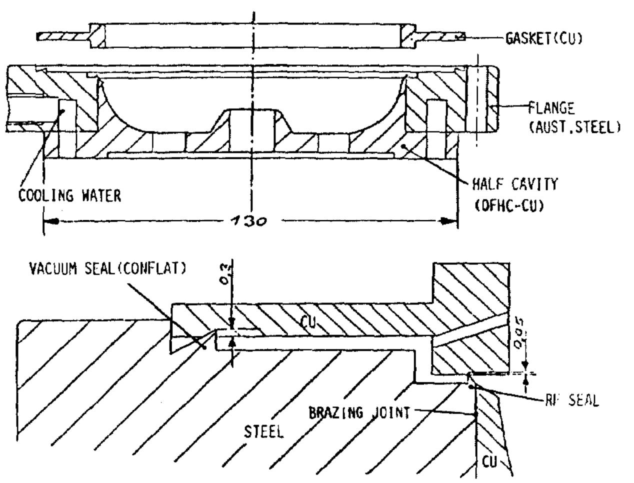

Fig.5: The vacuum-rf-seal for the sections of stage II

As a countermeasure against BBU ([7],[14]) the angle between adjacent pairs of coupling slots in the accelerating cavities is varied from 90° to 0° in steps of 8°; as a surprising consequence not only these cavities had to be tuned individually ($\Delta\nu \leq +0.4$ MHz), but also the coupling cavities ($\Delta\nu \leq -1.3$ MHz) because of a change of second nearest neighbour coupling. The effective shunt impedance of the sections turned out as 68±2 MΩ/m and with only circumferential cooling they were powered up to 17 kW/m.
A schematic plot of the rf-system is given in Fig. 6. The combined power of the two TH 2075-klystrons can be variably distributed between stages I and II according to their different beam loading by a phase shifter on the low power side of one klystron. The common power supply (2*25 kV/3.1 A) has only a modest filtering (1.5 H, 2μF), thus allowing to protect the klystrons just by series resistors of 100 Ω. A voltage of 0-600 V between the bodies and the isolated collectors of the TH 2075 counterbalances the ripple of 1%/600 Hz of the power supply. A feedback loop acting simultaneously on the phase shifter and this body-collector-voltage results in a rf-amplitude in stage I and II constant to better than ±0.1%.
The more than thirty parameters and limits of the rf-system are supervised by a microprocessor controlled interlock-system [15], which in addition is connected to the HP 1000 computer of the MAMI control system.
A peculiarity of the waveguide system is the use of circular magic T's; Fig. 7 shows one of these elements: with input power at port 1 and a load at port 2 it serves as a 3 dB divider; with input power a port 1 and 2 it is a variable power combiner/divider to port

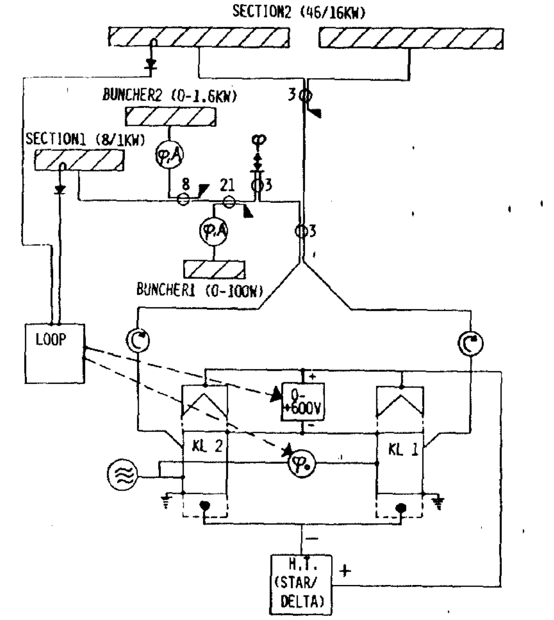

Fig. 6: The rf-system of MAMI A (schematic)

3 and 4, the division ratio changing with the phase difference between the inputs. The match at the transition from rectangular to circular waveguide is mainly done by the diameter of the latter. By other angles between the ports any desired coupling resp. isolation can be set easily.

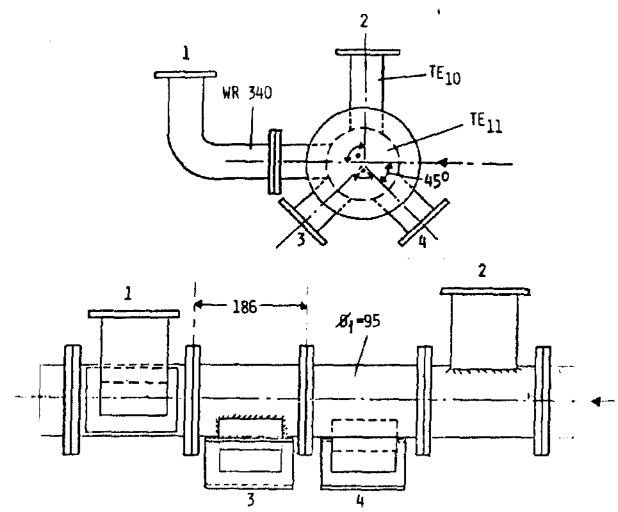

Fig. 7: A circular magic T power combiner/divider

Beam Monitoring System.

The beam monitors of the 2nd stage are compiled in Tab. 2. Monitors A und B are improved versions of the ones used in the first stage [1],[9],[16]. The latter, due to their high Q-value, suffer from overload at high beam intensity [6]. So, for the 2nd stage low Q monitoring-resonators had been developed with even improved sensitivity [17]. Monitor C is used for an interlock to prevent damage from excessive beam loss in the microtron. It consists of a pair of ferrite toroid current monitors which are sensitive to the 10 nsec blackout marks in the c.w. beam [1]. Located at input and output of the microtron vacuum system (F in fig. 3) they compare input and output beam intensity and switch off the beam if the difference becomes to large.

	Quantity measured	Location	Principle
A)	position	linac axis	resonator E_{110}
B)	intensity and phase	linac axis	resonator E_{010}
C)	intensity	input and output of microtron	ferrite
D)	position and profile	interface	wire scanner
E)	position and profile	extraction-chamber	wire scanner
F)	cross section	magnet-chamber	sychrontron radiation

Tab. 2: Beam monitors in the 2nd stage of MAMI

Monitors D are wire scanners identical to the ones used in the first stage [18]. Their locations are marked "SC" in fig. 2.
Monitor E consists of a row of 50 wire scanners, located inside the extraction chamber. They are moved through all beams simultaneously immediately downstream the return pipes. This monitor is expected to be a useful tool for beam matching by computer and for investigation of methods to compensate the effect of small range magnetic field errors [19].

Monitor F shows the beam shapes in the right hand magnet chamber (fig. 3) by means of the synchrotron radiation. The very simple setup shown in fig. 8, forming a compromise between beam separation and freedom of dispersion, provides good information also on horizontal phase space [20]. A system of four mirrors arranges the beam images into four lines on a TV monitor (s. fig. 9b), starting at the 13th orbit. The sizes of these mirrors are choosen different in order to partly cancel the increase of brightness with energy. This monitor shows the beam cross sections very well at a few μA of beam intensity already and thus has proven to be a very valuable tool for the beam setup procedure.

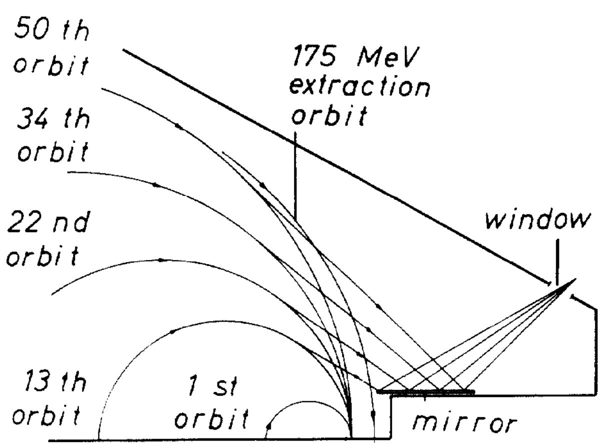

Fig. 8: Layout of the synchrotron light monitor

Data Acquisition and Control

Meanwhile the data acquisition and control system for MAMI has grown not only by a number of CAMAC modules (now altogether 5 crates) and additional electronic equipment, but also by intelligence: Where possible, microprocessors were used to replace complex electronics and implement new functions. One example is the new knob-system capable of handling up to 16 quasianalogue data entry units, others are the rf-interlock-system and the multichannel power supply described below. As the general configuration of the system was already discussed in some detail in [8], only a few remarks on supplementary equipment for the 175 MeV stage are given here.

μp-controlled 256 channel steering magnet supply

A new μp controlled multichannel power supply was developed to supply 256 steering and quadrupole magnets in the microtron and the beam guiding systems. The μP corrects the offset of each channel and controls the current and voltage values in order to detect short circuits in coils and bad cable connections. Defective channels will cause a LAM in the CAMAC system.
The system uses one 12 bit DAC, the output of which is multiplexed to 256 S+H units. These serve as reference for the bipolar power outputs, each of which can supply up to 3.5 A into a 2 Ω load.

Parallel data acquisition for the rf monitor signals: Using the new monolithic 6 bit flash-ADC's (Siemens SDA5010, conversion time 10 nsec) available on the market since 1981, a fast 8 bit parallel data acquisition system for the rf monitor signals has been built at reasonable costs. The 6 monitor signals of each stage are multiplexed to 6 ADC's working in parallel. The converted data of the individual turns are then stored continuously in fast ECL RAMs (the time delay between the first pulses is only 13.5 nsec). A programmable triggergenerator (about 1 nsec resolution) provides the correct trigger pulse train similar to the sequence of diagnostic pulses from the rf-cavities of the microtron. The system will soon be connected to the computer to allow for automatic optimization of both MAMI stages [9].

Injection: Since the move to the new control room, also the Van de Graaff injector is operated through the computer. A high resolution DAC provides the reference voltage for the generating voltmeter and thereby for the belt charge electronics. A multiplexer gives access to the motor driven rotary axes which control the state of the gun and the chopper power. The actual parameters are read via CAMAC-Scanning ADC and scalers.

The MAMI Control System Software

The principal structure and design goals of the software for the MAMI control system have been desribed elsewhere [8]. The last year had to show, whether the design objectives stated in [8] really held the intention of the sytem architecture, since this was the time to incorporate the second stage of the microtron into the control system.

First of all the data base had to be extended to be able to hold information about all additional elements of the second stage (about 250 elements). Secondly, new handlers and service routines had to be written for new types of equipment to be supported by the control system. In the following we describe some of these shortly.

Control of the van de Graaff preaccelerator: To interface to the newly developed hardware described above, a series of software modules had to be written. Now, the touchpanel and knobs [8] allow the user to control interactively the van de Graaff parameters (Wehnelt voltage, heating current, chopper amplitude, high voltage, and generating-voltmeter (GVM) voltage) via standard software modules. More 'intelligent' routines facilitate some more complex procedures like shutting down or conditioning.

Control and supervision of the rf-system: As there had been built a new rf-system all service-routines had to be re-written. Now all functions (rf on/off, amplitude and phase of each acceleration-section) can be done via computer (touch panel and knobs). Important design considerations were to generate understandable messages to the operator's terminal about hardware failures, and, further, that even on errors by the operator no component of the rf-system could be damaged (e.g. speed limit for rf-amplitude). Important is that an interlock system, controlled by a microprocessor, switches off the rf-supply if limits are exceeded and informs via a CAMAC link the operator at his console. In addition, it is possible to calculate the efficiency of the klystrons by measuring the temperature of the cooling water (in/out) and compare it with the incoming power of the klystrons. If the difference is too large, the operator will be informed and if necessary, the rf-power will be switched off automatically.

Other newly developed routines serve for the control of the dipoles of the second stage (including 'cycling', and 'ramping' to the appropriate field values) and for support of the high resolution steering magnets supply. In addition some consolidation work had to be done, mainly concerning the thorough checking and reporting of error conditions.

It turned out that indeed the initial design of the control system software allowed all the necessary changes and additions be done very easily. An additional proof for the quality of the original design is that only one of the original software designers and programmers is still working in this project, all other people started programming for the MAMI control system in 1982.

The loosely coupled two computer system (2 HP1000 computers communicating via a hardwired link using interprocess communications and sharing a common file system) proved to be capable to perform the additional tasks with only minor configuration changes. It was only necessary to add more memory to both computers to reduce the contention for memory of the various processes.

First Operational Experience

In the first test runs by end of January 1983 the beam persistently stopped after the 40th linac traversal and it turned out that some spacers in the vacuum chamber K1 (see fig. 3) had changed their position. Fortunately, it was possible to repair this in situ with relatively little dismantling. So the next test could be run in Feb. 17th and it was possible to accelerate the beam to full energy. One week later, after some additional alignment and minor repairs, a beam transmission to full energy in excess of 94% had been achieved, as measured by the beam intensity monitor resonator on the linac axis (see fig. 9a).

In these tests, however, the beam could not be extracted from the machine because installation of the exterior beam guiding systen had not yet been finished.* For this reason the c.w. beam intensity was limited to a few microamps, since, without extraction, the beam was dumped somewhere in the vacuum chamber after a 52nd linac traversal (therefore the intensity signal in fig. 9a shows 52 peaks). The fact, however, that the beam transmission is measured using the 10 nsec diagnostic pulses demonstrate that at least beam emittance is not a notable limitation for transmission.

In a further test run it was tried sucessfully to change the beam energy by multiplying all settings by a common factor. It was possible to raise the energy to 187 MeV after the 51st traversal (so, actually, the beam was dumped at 190 MeV). The energy was limited by the control range of the main magnet power supply.

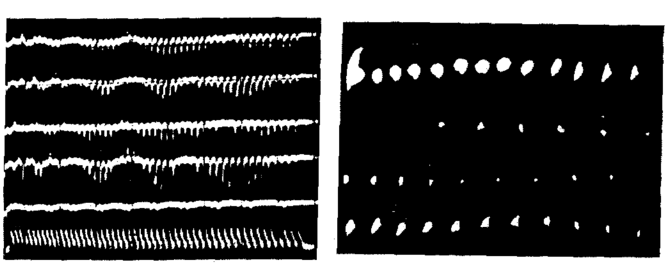

Fig.9: Monitorsignals from the 175 MeV stage (s. text)

Fig. 9a shows the signals from the beam monitors on the linac axis of one of these runs. The 1st and 2nd line show horizontal and vertical beam position respectively upstream the linac, 3rd and 4th line resp. downstream the linac. 5th and 6th line show phase and intensity upstream the linac. It is seen, that, at this specific run, the longitudinal tune was about 1/5. Actually, about equally stable operation was obtained at any tune within the range 1/5 to 1/4 (design value is 0.23).

Fig. 9b shows the TV-viewscreen of the synchrotron monitor. The numbers refer to the linac traversals, increasing traversal numbers go from the right to the left. The seamingly increase of the beam size with traversal number in each line is just a matter of overexposure of the photograph.

Acknowledgements

We are highly indepted to all technical staff members, of our institute who participated in design and construction of MAMI. Without their cooperative engagement it would not have been possible to contruct MAMI as a really in-house built machine, not to speak of keeping the tight time schedule of last year.

References

[1] H. Herminghaus et al., Nucl. Instr. & Meth. 138(1976)1

[2] Jahresbericht Institut für Kernphysik Mainz 1979

[3] U.E.P. Berg et al. Proc. Int. Symposium on Highly Excited States in Nuclear Reactions, Osaka, Japan, May 1980

[4] M. Begemann et al., Nucl. Instr. & Meth. 201(1982)287

[5] H. Herminghaus, K.H. Kaiser, U. Ludwig, Nucl. Instr. & Meth. 187(1981)103

[6] H. Aufhaus et al., Proc. of the 1981 Linear Accelerator Conference, Santa Fe, N.M., LA-9234-C, p. 22

[7] H. Euteneuer, H. Herminghaus, R. Klein l.c. p. 239

[8] H. v.d.Schmitt, H. Aufhaus, l.c. p. 274

[9] H.J. Kreidel, K. Merle, l.c. p. 245

[10] U. Ludwig, Inst. f. Kernphysik, Univ. Mainz, Int. Note MAMI 5/80

[11] Jahresbericht Inst. f. Kernphysik, Mainz 1980/81

[12] S.O. Schriber et al., Proc. of the 1976 Proton Linear Acc. Conf., Chalk River, AECL-5677, p.338, p. 405

[13] H. Schöler, H. Euteneuer, Inst. f. Kernphysik, Univ. Mainz, Int. Note MAMI 4/82

[14] H. Herminghaus, H. Euteneuer, Nucl. Instr. & Meth. 163(1979)299

[15] M. Loch, Inst. f. Kernphysik, Univ. Mainz, Int. Note MAMI 9/82

[16] B. Mertin, Diplomathesis, Inst. f. Kernphysik, Univ. Mainz, KPH 5/80

[17] H. Herminghaus, Inst. f. Kernphysik, Univ. Mainz, Int. Note MAMI 8/80

[18] H. Aufhaus, Doctoral thesis, Inst. f. Kernphysik, Univ. Mainz, KPH 35/81

[19] H. Herminghaus, Inst. f. Kernphysik, Univ. Mainz, Int. Note MAMI 2/80

[20] H. Herminghaus, Inst. f. Kernphysik, Univ. Mainz, Int. Note MAMI 8/81

*On March 21, during the conference, a 15 microamps c.w. beam had been extracted and delivered to the switch hall.

The work was supported in part by "Deutsche Forschungsgemeinschaft".